Converting normal insulators into topological insulators via tuning orbital levels

Wu-Jun Shi,[1,2] Junwei Liu,[3] Yong Xu,[1,4,5,*] Shi-Jie Xiong,[2] Jian Wu,[1,4] and Wenhui Duan[1,4,†]

[1]*State Key Laboratory of Low-Dimensional Quantum Physics, and Department of Physics,
Tsinghua University, Beijing 100084, People's Republic of China*
[2]*National Laboratory of Solid State Microstructures, and Department of Physics, Nanjing University,
Nanjing 210093, People's Republic of China*
[3]*Department of Physics, Massachusetts Institute of Technology, Cambridge, Massachusetts 02139, USA*
[4]*Collaborative Innovation Center of Quantum Matter, Tsinghua University, Beijing 100084, People's Republic of China*
[5]*Department of Physics, McCullough Building, Stanford University, Stanford, California 94305-4045, USA*

Tuning the spin-orbit coupling strength via foreign element doping and modifying bonding strength via strain engineering are the major routes to convert normal insulators to topological insulators. We here propose an alternative strategy to realize topological phase transition by tuning the orbital level. Following this strategy, our first-principles calculations demonstrate that a topological phase transition in the cubic perovskite-type compounds $CsGeBr_3$ and $CsSnBr_3$ could be facilitated by carbon substitutional doping. Such a unique topological phase transition predominantly results from the lower orbital energy of the carbon dopant, which can pull down the conduction bands and even induce band inversion. Beyond conventional approaches, our finding of tuning the orbital level may greatly expand the range of topologically nontrivial materials.

Topological insulators (TIs), as new quantum states of materials characterized by insulating bulk and metallic surface states that are topologically protected against backscattering, have attracted enormous interest in recent years due to their novel electronic properties [1,2]. So far many TI materials have been theoretically predicted and/or experimentally identified, including HgTe quantum wells [3,4], Bi_2Se_3-class TIs [5–7], $TlBiSe_2$ TIs [8], half-Heusler TIs [9], etc. All of these materials inherently have an inverted band structure and thus are topologically nontrivial. However, there exists a much wider range of other materials which intrinsically are topologically trivial but potentially can be changed into TIs. Such a large class of materials, if applicable for TI-related research and applications, would greatly facilitate the development of condensed-matter physics and materials science.

How to convert conventional materials (or more specifically, semiconductors) into TIs is a crucial problem yet to be solved. A few approaches have been proposed and developed for the purpose. For example, topological phase transitions in normal insulators can be induced by manipulating the crystal lattice via external strain [10–15] and chemical doping or functionalization [16–22], or by tuning the electronic structure via electric field [23] and quantum confinement [24]. The general physical picture behind these approaches is either to tune the spin-orbit coupling (SOC) strength or to change the bonding strength of the normal insulators, so as to induce the band inversion required.

In this work, we reveal an alternative, physically distinct approach to achieve TI states from conventional materials, where doping heavy elements with large SOC strength and applying large strain are not requisite any more. Based on the tight-binding Hamiltonian and first-principles calculations, we demonstrate that topological phase transition of normal

insulators can be successfully realized by tuning the orbital levels (rather than SOC strength) via doping. This topological phase transition is originated from the difference in orbital levels between the host and dopant atoms. As examples, we show that the perovskite-type compounds $CsGeBr_3$ and $CsSnBr_3$ can be converted from normal insulators to three-dimensional (3D) strong TIs by substituting Ge or Sn with C. The lower p orbital level of C ($2p$) than that of Ge ($4p$) or Sn ($5p$) pulls down the conduction bands and could lead to an interchange between the original conduction-band minimum (CBM) and valance-band maximum (VBM), i.e., these normal insulators are converted to TIs.

We first consider a generic tight-binding Hamiltonian:

$$\mathcal{H} = \sum_{\mu \vec{R}} \epsilon_\mu c_{\vec{R}}^{\mu\dagger} c_{\vec{R}}^{\mu} + \sum_{\mu\nu\vec{R}\vec{R}'} t_{\vec{R}\vec{R}'}^{\mu\nu} c_{\vec{R}}^{\mu\dagger} c_{\vec{R}'}^{\nu} + \sum_{\vec{R}} \lambda_{\vec{R}} \vec{L}_{\vec{R}} \cdot \vec{s}_{\vec{R}},$$

where ϵ_μ is the on-site energy of orbital μ; $c_{\vec{R}}^{\mu\dagger}$ ($c_{\vec{R}}^{\mu}$) is the fermion creation (annihilation) operator of orbital μ at site $\vec{R}$; $t_{\vec{R}\vec{R}'}^{\mu\nu}$ is the hopping integral between orbital μ at site $\vec{R}$ and orbital ν at site $\vec{R}'$; and $\lambda_{\vec{R}}$ is the SOC strength. From the tight-binding view, the electronic band structures are determined by the on-site energy ϵ, the hopping integral t, and the SOC strength λ. Therefore, the topological phase transition may be realized by tuning these three parameters of certain normal insulators. Actually it has been extensively shown that doping heavy atoms can be used to increase the SOC strength [18–20] or doping lighter atoms can be used to decrease the SOC strength, as demonstrated in the example of doping Bi with Sb [21], while applying external strain can change the interatomic distances which can affect the atomic wave function overlap and also the hopping integrals [11–13,16,17]. In contrast, herein, we focus on the role of the on-site energy change (by chemical doping) in the topological phase transition. Figure 1 schematically shows the relevant topological phase transition mechanism: due to the difference in orbital level (i.e., the on-site energy) between the

---

*yongxu@mail.tsinghua.edu.cn
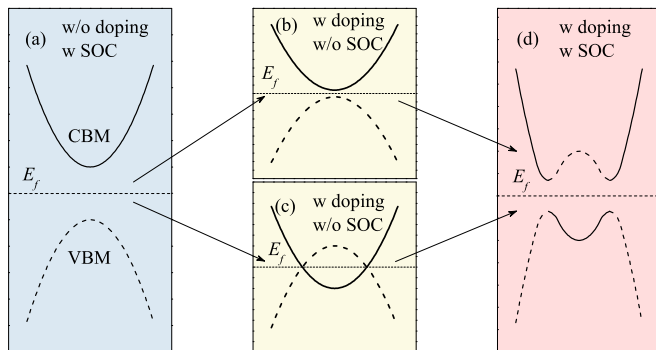†dwh@phys.tsinghua.edu.cn

FIG. 1. (Color online) Schematic illustration of the doping and SOC induced band inversion. (a) The original bands are not inverted. (b, c) The CBM and VBM shift toward each other induced by doping is less/larger than the band gap in (a). Note that a band inversion occurs in (c). (d) The final bands are inverted. For the path (a)-(b)-(d), the doping reduces the band gap, and the SOC induces the band inversion, while for path (a)-(c)-(d) the doping induces the band inversion, and the SOC opens a band gap. The solid and dashed curves denote the sub-bands that have opposite parities. The Fermi level (E_f) is denoted by the dashed line.

substitutional dopant and host atoms, the CBM and VBM shift towards each other owing to doping, causing a reduction or even disappearance of the band gap; SOC then further induces a band inversion or band-gap reopening.

In order to prove the above strategy, we perform the first-principles calculations. As is well known, in the ABX_3-type perovskite structures, the electronic states near the Fermi level are mainly contributed by the B-site and X-site atoms [11,25]. Therefore, these perovskite structures with the B-site or X-site substitution by foreign atoms with different orbital levels are suitable to tune the bands near the Fermi level [25]. Herein, the halide perovskite-type compounds $CsGeBr_3$, and $CsSnBr_3$, which might be converted into topological states under external strain [10,11], are selected to demonstrate the concept.

It is worthwhile to note that halide perovskite-type compounds can exhibit rich structural phases under different conditions of pressure and temperature. The low-temperature phase of $CsGeBr_3$ is rhombohedral [26] and that of $CsSnBr_3$ is tetragonal, or monoclinic [27,28]. All these materials will transit into the cubic phase when increasing temperature. The transition temperature T_C is ~ 510 K for $CsGeBr_3$ [26], and is around room temperature (~ 292 K) for $CsSnBr_3$ [27,28]. In fact, a lower T_C could be achieved by applying an external pressure. For instance, the cubic phase becomes stable at room temperature under an external pressure of ~ 1 GPa [26]. On the other hand, a structural phase that is originally metastable in its freestanding form could be stabilized when grown on the substrate, as shown by a recent experiment of SnSe on Bi_2Se_3 substrate [29]. Thus, for the sake of simplicity and without loss of generality, we only consider the cubic phase of $CsGeBr_3$ and $CsSnBr_3$ in the following.

The first-principles calculations are performed using the Vienna *ab initio* simulation package (VASP) [30] with the plane-wave basis. The interactions between the valence electrons and ion cores are described by the projector augmented wave method [31], and exchange-correlation potential is

TABLE I. The PBE calculated equilibrium lattice constant (a_0); global band gap without SOC (E_g) and with SOC (E_g^{soc}); and band gap (E_{trim}^{soc}) at the R (pure) or Γ (doped) point of pure $CsGeBr_3$, pure $CsSnBr_3$, $CsGe_{0.875}C_{0.125}Br_3$, and $CsSn_{0.875}C_{0.125}Br_3$. "$-$" presents the inverted band gap.

	a_0 (Å)	E_g (meV)	E_g^{soc} (meV)	E_{trim}^{soc} (meV)
$CsGeBr_3$	5.604	745.2	583.4	583.4
$CsGe_{0.875}C_{0.125}Br_3$	11.085	0.8	-16.1	-31.6
$CsSnBr_3$	5.883	625.9	279.2	279.2
$CsSn_{0.875}C_{0.125}Br_3$	11.578	0.0	-16.1	-35.3

formulated by the generalized gradient approximation with the Perdew-Burke-Ernzerhof (PBE) scheme [32]. The Heyd-Scuseria-Ernzerhof (HSE) [33] hybrid functional is employed to check the results. The Γ-centered k points are used for the first Brillouin-zone sampling. The plane-wave basis cutoff energy is set to 500 eV. The structures are optimized until the forces on atoms are less than 5 meV/Å. For pure $CsGeBr_3$ and $CsSnBr_3$, a dense $10 \times 10 \times 10$ grid of k points is used. To simulate doping effect, a $2 \times 2 \times 2$ supercell is employed with one Ge or Sn substituted by one C ($CsGe_{0.875}C_{0.125}Br_3$ or $CsSn_{0.875}C_{0.125}Br_3$), and a $5 \times 5 \times 5$ grid of k points is used. The fully relaxed lattice constants of pure and doped structures are listed in Table I, and will be used in subsequent calculations. Note that the lattice constants of pure structures are consistent with the values in Ref. [10].

First, we analyze the electronic structure and topological properties of $CsGeBr_3$ and $CsSnBr_3$. As an example, the calculated band structures of $CsGeBr_3$ are shown in Fig. 2. It can be seen that without SOC $CsGeBr_3$ has a direct band gap at the R point [Fig. 2(a)]. A further analysis of the wave functions and their symmetries reveals that the VBM states consist of Br $4p$ and Ge $4s$ states and possess the R_1^+ symmetry with even
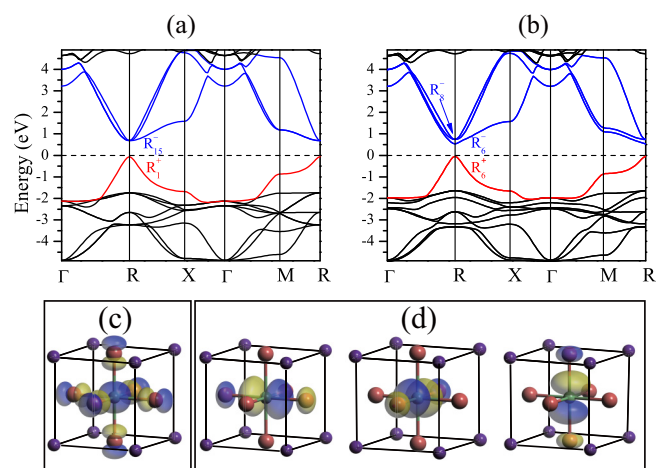

FIG. 2. (Color online) The calculated band structures of pure $CsGeBr_3$ without (a) and with (b) SOC; the real part of the wave functions of the R_1^+ (c) and R_{15}^- (d) states without SOC, the blue (yellow) isosurfaces represent the "$+$" ("$-$") sign of the wave functions. The Fermi level is set to zero and indicated by the dashed line.

parity [Fig. 2(c)], while the CBM states mainly come from Ge $4p$ and have R_{15}^- symmetry with odd parity [Fig. 2(d)]. By taking SOC into account [Fig. 2(b)], GsGeBr$_3$ is still a narrow-gap semiconductor with direct gap at the R point, while the R_{15}^- states (the CBM) split into twofold degenerate R_6^- states and fourfold degenerate R_8^- states, and the VBM has the twofold R_6^+ symmetry. Meanwhile, the band gap decreases from 745.2 to 583.4 meV (Table I). The electronic structures of CsSnBr$_3$ is similar to that of CsGeBr$_3$, except for the magnitude of the band gap (see Table I). By calculating the parities of all the occupied states at the time-reversal-invariant momentum (TRIM) points (i.e., Γ, R, X, and M points), we find that pristine CsGeBr$_3$, and CsSnBr$_3$ are trivial insulators with the same Z_2 index (0;000) based on parity criteria [34].

On the other hand, the opposite parities of the CBM and VBM at the R point suggest that it is possible to drive CsGeBr$_3$ and CsSnBr$_3$ into a topologically nontrivial phase. For CsGeBr$_3$, as shown in Fig. 2(d), the CBM states mainly come from the Ge $4p$ orbitals, while for CsSnBr$_3$ the CBM states mainly come from the Sn $5p$ orbitals. Therefore, the CBM can be pulled down by substituting the Ge or Sn atoms with foreign atoms that have the similar valence electron configuration as compared to Ge or Sn atoms but lower p orbital level than Ge or Sn atoms. Following this strategy, it is natural to use the C atom, which is at the same group as Ge and Sn atoms, as the substitutional dopant. Whereas the SOC strength of the C atom is smaller than those of Ge and Sn atoms, the C doping will reduce the total SOC strength of the system.

Our PBE calculations show that substitutional C doping can effectively decrease the band gap and induce a topological phase transition. The results of CsGe$_{0.875}$C$_{0.125}$Br$_3$ are presented in Fig. 3. It is worth noting that the original R point is folded into the Γ point because the $2 \times 2 \times 2$ supercell is adopted in the calculations. In this case, the VBM and CBM can be relabeled as Γ_1^+ and Γ_{15}^- states for convenience. After doping C atoms, as expected, the Γ_1^+ and Γ_{15}^- states move toward each other and the band gap decreases close to zero ($\sim$0.8 meV without SOC) as indicated in Fig. 3(a). Then we take SOC into account. As shown in Fig. 3(b), the SOC splits Γ_{15}^- states into Γ_8^- and Γ_6^- states and changes Γ_1^+ to Γ_6^+. More importantly, the SOC can further push the Γ_6^+ state up higher than Γ_6^- and even Γ_8^- states. The detailed evolution of all the states can be further clarified by artificially tuning the SOC strength (λ) in the calculations from the original SOC strength (λ_0). As shown in Fig. 3(c), without SOC, Γ_6^- and Γ_8^- states are degenerate and higher in energy than the Γ_6^+ state. By increasing the SOC strength, the splitting between Γ_6^- and Γ_8^- states increases, and Γ_6^+ is pushed up relatively. Across a critical point (i.e., $\lambda/\lambda_0 \sim 0.03$), the energy of Γ_6^+ will be higher than that of Γ_6^- and eventually exceed that of Γ_8^- when $\lambda/\lambda_0 > 0.4$. The band evolution with SOC implies that there exists a direct-band-gap closing and reopening, which is a solid signal of topological phase transition. To confirm this, we further calculate the products of parity eigenvalues of all the occupied bands at the TRIM points as shown in Fig. 3(d). According to the parity criteria [34], it is clear that the above band inversion only induces a sign change at the Γ point and causes the Z_2 topological index to be nontrivial (1;000).
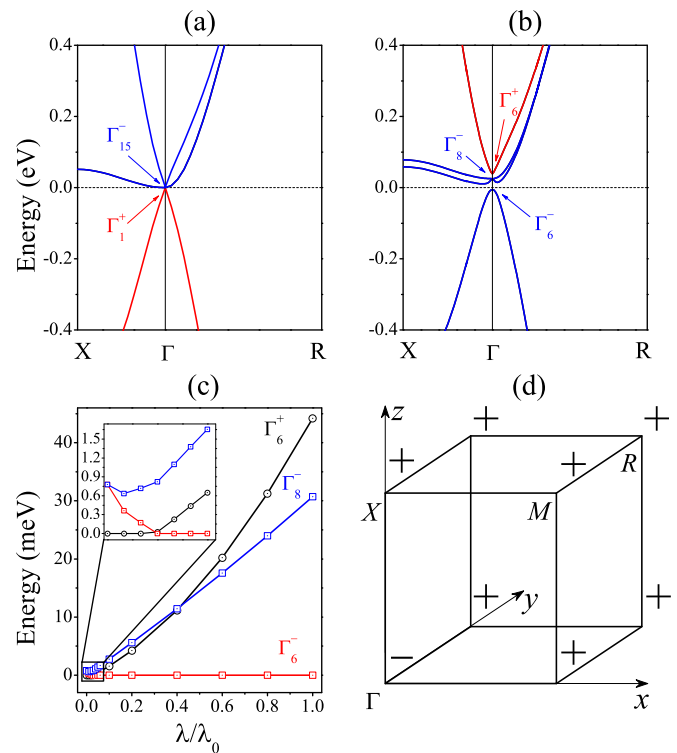

FIG. 3. (Color online) The PBE calculated electronic band structures of CsGe$_{0.875}$C$_{0.125}$Br$_3$ without (a) and with (b) SOC; the calculated energy level of Γ_6^+, Γ_6^-, and Γ_8^- states (c) as the artificial SOC strength (λ) increases from zero to original SOC strength (λ_0); and the diagrams depicting the signs of the products of parity eigenvalues of all the occupied bands at every TRIM point (d). The inset in (c) zooms into the band inversion between Γ_6^+ and Γ_6^-. In (a) and (b), the Fermi level is set to zero, and indicated by the dashed line.

The striking properties of 3D topological materials is the Dirac-type surface states in the bulk gap, which can be directly measured by angle-resolved photoemission spectroscopy (ARPES). Herein, we calculate the surface states of semi-infinite CsGe$_{0.875}$C$_{0.125}$Br$_3$ by surface Green's-function method based on the *ab initio* calculation [35–37]. The imaginary part of the surface Green's function is relative to the local density of states (LDOS), from which we can obtain the surface states. The calculated LDOS of the (100) surface is displayed in Fig. 4. We can clearly see that the topological surface states form a single Dirac cone at the Γ point. The Fermi velocity is about 1.45×10^5 m/s, which is of the same order of magnitude as those of Bi$_2$Te$_3$-type TIs [6].

For CsSnBr$_3$ with Sn substituted by C, the pictures are slightly different. Without SOC, the C doping induces a band inversion: the Γ_1^+ states are above the Γ_{15}^- states and the Fermi level crosses the Γ_{15}^- states, and therefore the materials are metallic (see Table I). Although the band inversion is not induced by the SOC, the SOC still plays an important role. Similar to the case of CsGe$_{0.875}$C$_{0.125}$Br$_3$, SOC will split Γ_{15}^- into Γ_8^- and Γ_6^- states and change Γ_1^+ to be Γ_6^+, which opens the band gaps around the Fermi level (see Table I) to drive the materials into topologically nontrivial phases. As confirmed by our Z_2 calculations, all these materials are 3D strong TIs.
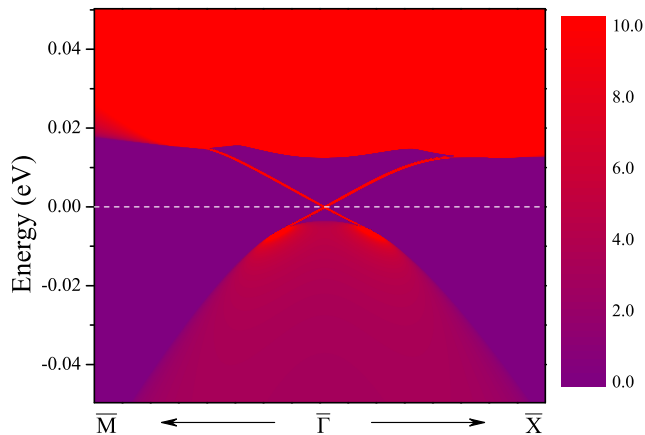
FIG. 4. (Color online) The calculated LDOS of $CsGe_{0.875}C_{0.125}Br_3$. The Fermi level is set to zero, and indicated by the dashed line. Clearly, Dirac surface states emerge in the bulk gap.

All the above results show that $CsGeBr_3$ with C doping undergoes topological phase transition through path (a)-(b)-(d), while the $CsSnBr_3$ with C doping undergoes topological phase transition through path (a)-(c)-(d) (see Fig. 1). Evidently the topological phase transition can be attributed to the lower orbital levels of C $2p$ states in comparison with Ge $4p$ or Sn $5p$ states, and different paths for the topological phase transition originate from the energy difference between the dopant state (i.e., C $2p$ state) and host state (i.e., Ge $4p$ or Sn $5p$ state) around the Fermi level. Larger difference in the orbital levels leads to larger downshift of the CBM, and the band inversion occurs directly when the energy difference is large enough.

In general, doping smaller atoms will inevitably decrease the lattice constant and have a similar effect as a compressive strain, which may induce the topological phase transition in some cases [11]. Thus we perform other comparative calculations to provide a full picture of the effects of C doping. When we shrink the lattice constant of $CsGeBr_3$ from the equilibrium lattice of pure $CsGeBr_3$ (5.604 Å) to that of $CsGe_{0.875}C_{0.125}Br_3$ (5.543 Å), the band gap deceases by about 150 meV with or without SOC. On the other side, if we only dope C atoms but fix the lattice constant to the equilibrium lattice of pure $CsGeBr_3$, the band gap decreases by about 630 meV without SOC and 490 meV with SOC, which is still in the topologically trivial phase. The different changes of band gap with and without SOC are due to the smaller SOC strength of C atoms than that of Ge atoms. According to the above comparison, the topological phase transition comes from the combined effects of on-site energy tuning and the lattice shrinkage, while the changes of on-site energy play a dominant role. Similar calculations for $CsSn_{0.875}C_{0.125}Br_3$ show that even without lattice shrinkage the band inversion can occur. This again indicates the dominant role of tuning the on-site energy in the topological phase transitions. Note that the substitutional C atoms might shift towards the neighboring Br atoms to increase the C-Br interaction. The resulting structural distortion, though leading to band splittings due to the break of the lattice symmetry, would not affect the band inversion.

TABLE II. The HSE calculated band gap at the R (Γ) point without SOC (E_g^{HSE}) and with SOC ($E_g^{HSE-soc}$) of pure $CsGeBr_3$ and $CsSnBr_3$ ($CsGe_{0.875}C_{0.125}Br_3$ and $CsSn_{0.875}C_{0.125}Br_3$). "−" presents the inverted band gap.

	E_g^{HSE} (meV)	$E_g^{HSE-soc}$ (meV)
$CsGeBr_3$	1246.5	1068.2
$CsGe_{0.875}C_{0.125}Br_3$	363.3	318.1
$CsGe_{0.875}C_{0.125}Br_3$[a]	0.0	−64.5
$CsSnBr_3$	1302.8	927.8
$CsSn_{0.875}C_{0.125}Br_3$	17.6	−62.2

[a]With 7% volume decreasing.

It is well known that PBE usually underestimates the band gap due to the self-interaction error. Specifically, the band gap of cubic $CsGeBr_3$ is 1.59 eV (at 300 K under 1.2-GPa pressure) as measured by optical absorption [26]. The band gap of $CsSnBr_3$ is 1.80 eV (0.34 eV) for the cubic phase at 300 K as obtained from optical (transport) experiments [28]. The PBE calculated band gaps of the cubic-phase $CsGeBr_3$ and $CsSnBr_3$ are 583.4 and 279.2 meV (including the spin-orbit coupling), respectively (see Table I). We employ the HSE functional to check the band-gap issue. For the $CsGeBr_3$ and $CsSnBr_3$ with SOC, the HSE predicted band gaps are 1068.2 and 927.8 meV, respectively. Although they are still smaller than the experimental values and GW calculated results [38], they are much improved over PBE calculated ones. For $CsGe_{0.875}C_{0.125}Br_3$ and $CsSn_{0.875}C_{0.125}Br_3$, the HSE calculated band gaps are 318.1 and −62.2 meV (the negative sign denotes a band inversion), respectively. This suggests that $CsSn_{0.875}C_{0.125}Br_3$ is a TI, while $CsGe_{0.875}C_{0.125}Br_3$ is not. Despite the fact that $CsGe_{0.875}C_{0.125}Br_3$ is topologically trivial, the substitution of Ge with C shifts the CBM downward significantly. Applying an external pressure could help drive $CsGe_{0.875}C_{0.125}Br_3$ into TI. The HSE calculations predict that the band order would get inverted if decreasing the material volume by 7%, and a −64.5-meV band gap is obtained when including the SOC (see Table II). From the above PBE and HSE calculations, one knows that even using the advanced methods there could exist a discrepancy in the band gap between the prediction and the reality, and an accurate description of band gap is quite challenging and beyond the scope of the present work. However, importantly, by using different exchange-correlation functionals we get the same physical picture that the substitution of Ge or Sn with C tunes orbital levels and thus facilitates a band inversion, validating the concept we proposed. Note that the band gap at the Γ point predicted by HSE is $\sim$20 meV larger than that by PBE (see Tables I and II). This is presumably because the (partial) correction of the self-interaction error in HSE, which may lead to relatively more localized electronic states than PBE, could give a stronger effective SOC.

It should be noticed that the temperature effects are important to the present system. As the band gap of the TI phase is on the order of the room-temperature thermal excitation energy of 26 meV, the thermal excitation would affect transport properties of metallic surface states by some extent. Nevertheless, the existence of massless Dirac fermions on the surface, as a hallmark of topological insulators, is

expected to be detectable by ARPES. Another intriguing feature must be mentioned: lowering the temperature could result in a TI to normal insulator transition, as caused by a temperature-induced structural phase transition which can increase the band gap. This unusual feature will be discussed later in detail in our future work.

Based on the general tight-binding picture, it is expected that the heavy elements doping can also induce the topological phase transition by pulling up the VBM and increasing the SOC strength in some materials. Furthermore, our strategy of tuning the onsite energy is not limited for 3D TIs. As is well known, the band inversion also has a similar fundamental effect on weak TIs, topological crystalline insulators [39–41], the quantized anomalous Hall insulators [42,43], and other topological systems. For all those systems, in principle, we can tune the on-site energy by doping and make them nontrivial.

In summary, we propose a strategy of realizing topological phase transition by tuning orbital levels via chemical doping. Due to the different orbital levels of the dopant and the substituted host atoms, the dopant can affect the energy band around the Fermi level and can reduce the band gap effectively or even induce a band inversion, and can promote the topological phase transition.

[1] M. Z. Hasan and C. L. Kane, Rev. Mod. Phys. **82**, 3045 (2010).

[2] X.-L. Qi and S.-C. Zhang, Rev. Mod. Phys. **83**, 1057 (2011).

[3] B. A. Bernevig, T. L. Hughes, and S.-C. Zhang, Science **314**, 1757 (2006).

[4] M. König, S. Wiedmann, C. Brüne, A. Roth, H. Buhmann, L. W. Molenkamp, X.-L. Qi, and S.-C. Zhang, Science **318**, 766 (2007).

[5] H. Zhang, C.-X. Liu, X.-L. Qi, X. Dai, Z. Fang, and S.-C. Zhang, Nat. Phys. **5**, 438 (2009).

[6] Y. L. Chen, J. G. Analytis, J.-H. Chu, Z. K. Liu, S.-K. Mo, X. L. Qi, H. J. Zhang, D. H. Lu, X. Dai, Z. Fang, S.-C. Zhang, I. R. Fisher, Z. Hussain, and Z.-X. Shen, Science **325**, 178 (2009).

[7] Y. Xia *et al.*, Nat. Phys. **5**, 398 (2009); D. Hsieh *et al.*, Nature (London) **460**, 1101 (2009).

[8] B. Yan *et al.*, Europhys. Lett. **90**, 37002 (2010); H. Lin, R. S. Markiewicz, L. A. Wray, L. Fu, M. Z. Hasan, and A. Bansil, Phys. Rev. Lett. **105**, 036404 (2010); T. Sato, K. Segawa, H. Guo, K. Sugawara, S. Souma, T. Takahashi, and Y. Ando, *ibid.* **105**, 136802 (2010); K. Kuroda *et al.*, *ibid.* **105**, 146801 (2010).

[9] S. Chadov, J. Liu, Nature Mater. **9**, 541 (2010); H. Lin *et al.*, *ibid.* **9**, 546 (2010); D. Xiao, Y. Yao, W. Feng, J. Wen, W. Zhu, X. Q. Chen, G. M. Stocks, and Z. Zhang, Phys. Rev. Lett. **105**, 096404 (2010).

[10] K. Yang, W. Setyawan, S. Wang, M. B. Nardelli, and S. Curtarolo, Nat. Mater. **11**, 614 (2012).

[11] H. Jin, J. Im, and A. J. Freeman, Phys. Rev. B **86**, 121102 (2012).

[12] J. Liu, Y. Xu, J. Wu, B.-L. Gu, S. B. Zhang, and W. Duan, Acta Cryst. C **70**, 118 (2014).

[13] L. Zhao, J. Liu, P. Tang, and W. Duan, Appl. Phys. Lett. **100**, 131602 (2012).

[14] A. Bera, K. Pal, D. V. S. Muthu, S. Sen, P. Guptasarma, U. V. Waghmare, and A. K. Sood, Phys. Rev. Lett. **110**, 107401 (2013).

[15] W. Feng, D. Xiao, J. Ding, and Y. Yao, Phys. Rev. Lett. **106**, 016402 (2011); W. Feng, W. Zhu, H. H. Weitering, G. M. Stocks, Y. Yao, and D. Xiao, Phys. Rev. B **85**, 195114 (2012); J.-J. Zhou *et al.*, Nano Lett. **14**, 4767 (2014); P. Tang, P. Chen, W. Cao, H. Huang, S. Cahangirov, L. Xian, Y. Xu, S. C. Zhang, W. Duan,

and A. Rubio, Phys. Rev. B **90**, 121408(R) (2014); H. Huang, J. Liu, and W. Duan, *ibid.* **90**, 195105 (2014).

[16] Y. Xu, B. Yan, H.-J. Zhang, J. Wang, G. Xu, P. Tang, W. Duan, and S.-C. Zhang, Phys. Rev. Lett. **111**, 136804 (2013).

[17] C. Si, J. Liu, Y. Xu, J. Wu, B.-L. Gu, and W. Duan, Phys. Rev. B **89**, 115429 (2014).

[18] S. Y. Xu, Y. Xia, L. A. Wray, S. Jia, F. Meier, J. H. Dil, J. Osterwalder, B. Slomski, A. Bansil, H. Lin, R. J. Cava, and M. Z. Hasan, Science **332**, 560 (2011).

[19] G. A. Fiete, Science **332**, 546 (2011).

[20] L. Wu, R. V. Aguilar, M. Brahlek, A. V. Stier, Y. Lubashevsky, C. M. Morris, L. S. Bilbro, N. Bansal, S. Oh, and N. P. Armitage, Nat. Phys. **9**, 410 (2013).

[21] H. J. Zhang, C. X. Liu, X. L. Qi, X. Y. Deng, X. Dai, S. C. Zhang, and Z. Fang, Phys. Rev. B **80**, 085307 (2009).

[22] C.-C. Liu, S. Guan, Z.-G. Song, S. Yang, J.-B. Yang, and Y. G. Yao, Phys. Rev. B **90**, 085431 (2014).

[23] H. Zhang, Y. Xu, J. Wang, K. Chang, and S.-C. Zhang, Phys. Rev. Lett. **112**, 216803 (2014).

[24] C. Liu, T. L. Hughes, X.-L. Qi, K. Wang, and S.-C. Zhang, Phys. Rev. Lett. **100**, 236601 (2008).

[25] W.-J. Shi and S.-J. Xiong, Phys. Rev. B **84**, 205210 (2011).

[26] U. Schwarz, F. Wagner, K. Syassen, and H. Hillebrecht, Phys. Rev. B **53**, 12545 (1996); D.-K. Seo *et al.*, Inorg. Chem. **37**, 407 (1998).

[27] M. Mori *et al.*, J. Phys. C **19**, 2391 (1986); D. E. Scaife *et al.*, J. Solid State Chem. **9**, 308 (1974).

[28] S. J. Clark *et al.*, J. Phys. Chem. Solids **42**, 133 (1981); I. Lefebvre, P. E. Lippens, M. Lannoo, and G. Allan, Phys. Rev. B **42**, 9174 (1990).

[29] Z. Wang, J. Wang, Y. Zang, Q. Zhang, J.-A. Shi, T. Jiang, Y. Gong, C.-L. Song, S.-H. Ji, L.-L. Wang, L. Gu, K. He, W. Duan, X. Ma, X. Chen, and Q.-K. Xue, Adv. Mater. **27**, 4150 (2015).

[30] G. Kresse and J. Furthmüller, Phys. Rev. B **54**, 11169 (1996).

[31] P. E. Blöchl, Phys. Rev. B **50**, 17953 (1994); G. Kresse and D. Joubert, *ibid.* **59**, 1758 (1999)

[32] J. P. Perdew, K. Burke, and M. Ernzerhof, Phys. Rev. Lett. **77**, 3865 (1996).

[33] J. Heyd, G. E. Scuseria, and M. Ernzerhof, J. Chem. Phys. **118**, 8207 (2003); J. Heyd and G. E. Scuseria, *ibid.* **120**, 7274 (2004).

[34] L. Fu and C. L. Kane, Phys. Rev. B **76**, 045302 (2007).

[35] I. Souza, N. Marzari, and D. Vanderbilt, Phys. Rev. B **65**, 035109 (2001).

[36] A. A. Mostofi, J. R. Yates, Y.-S. Lee, I. Souza, D. Vanderbilt, and N. Marzari, Comput. Phys. Commun. **178**, 685 (2008).

[37] M. P. Lopez Sancho, J. M. Lopez Sancho, J. M. L. Sancho, and J. Rubio, J. Phys. F **15**, 851 (1985).

[38] L.-Y. Huang and W. R. L. Lambrecht, Phys. Rev. B **88**, 165203 (2013).

[39] L. Fu, Phys. Rev. Lett. **106**, 106802 (2011).

[40] T. H. Hsieh, H. Lin, J. Liu, W. Duan, A. Bansil, and L. Fu, Nat. Commun. **3**, 982 (2012).

[41] J. Liu, T. H. Hsieh, P. Wei, W. Duan, J. Moodera, and L. Fu, Nat. Mat. **13**, 178 (2014).

[42] R. Yu, W. Zhang, H.-J. Zhang, S.-C. Zhang, X. Dai, and Z. Fang, Science **329**, 61 (2010).

[43] C.-Z. Chang, J. Zhang, X. Feng, J. Shen, Z. Zhang, M. Guo, K. Li, Y. Ou, P. Wei, L.-L. Wang, Z.-Q. Ji, Y. Feng, S. Ji, X. Chen, J. Jia, X. Dai, Z. Fang, S.-C. Zhang, K. He, Y. Wang, L. Lu, X.-C. Ma, and Q.-K. Xue, Science **340**, 167 (2013).